Structural determinations of homo and heterodi- or tetra-nuclear lanthanide complexes and their characterization by μ-Squid experiments

Jean-Pierre Costes, Carine Duhayon, Laure Vendier, Wolfgang Wernsdorfer

Structural determinations of homo and heterodi- or tetra-nuclear Lanthanide complexes and their characterization by μ-Squid experiments.

Jean-Pierre Costes,[a,b] , Carine Duhayon,[a,b], Laure Vendier,[a,b], Wolfgang Wernsdorfer[c,d]**

[a] *Laboratoire de Chimie de Coordination du CNRS, 205, route de Narbonne, BP 44099, F-31077 Toulouse Cedex 4, France*

[b] *Université de Toulouse ; UPS, INPT, F-31077 Toulouse Cedex 4, France*

[c] *Institute of Nanotechnology (INT), Karlsruhe Institute of Technology (KIT), Hermann-von-Helmholtz-Platz 1, D-76344 Eggenstein- Leopoldshafen, Germany.*

[d] *Institut Néel, CNRS / Université Grenoble Alpes, 25 rue des Martyrs, F-38000 Grenoble, France.*

Abstract

Two families of homo- and heterodinuclear complexes are prepared and structurally characterized, thus demonstrating that genuine complexes involving two lanthanide ions closely located in the lanthanide series can be obtained, taking into account a simple rule that necessitates introduction of the better Lewis acid Ln ion (the smallest Ln ion) into the inner coordination site of the main ligand used in this synthesis. In the first family, the presence of a deprotonated orthovanillin ligand (ovan) around the Ln ion positioned in the outer coordination site of the main ligand allows a good isolation of the dinuclear complexes. These complexes behave as SMSs when a Dy ion is coordinated in the outer site but a weak magnetic magnetic Ln-Dy interaction is needed to create a weak magnetic field able to suppress collapsing of the hysteresis loops in zero external applied field at very low temperature. In the second family, the ovan ligand is replaced by a chloride ligand, so that two dinuclear units are linked together by two Cl…HOMe hydrogen bonds to yield tetranuclear complexes that are not SMMs. Eventually these two preparation pathways are expected to give novel and genuine examples of homo or hetero-dinuclear and tetranuclear lanthanide complexes likely to furnish in future coordination complexes useful in quantum computing.

Introduction

The design of magnetic coordination complexes for quantum computing has been the source of a growing interest in the last decade[1-3]. The preparation of dinuclear complexes involving anisotropic metal ions in different environments and presenting a weak magnetic interaction is one among the synthetic methods retained for the preparation of such functional entities [4-8]. With use of a tripodal ligand, we want to show in the present paper that it is possible to isolate first homo and heterodinuclear lanthanide complexes and, in a second stage, to link two dinuclear entities through hydrogen bonds. We have previously shown that a tripodal ligand possessing two different coordination sites, an inner N_4O_3 and an outer O_3O_3 sites, was able to coordinate two Ln^{III} ions in order to yield homo and heterodinuclear complexes by a stepwise process [9]. So we have demonstrated, thanks to the positive Fast-Atom Bombardment technique (FAB^+), that pure genuine pure $Ln^{III}Ln'^{III}$ complexes can be isolated if the Ln^{III} ion introduced in the inner N_4O_3 coordination site has a greater Lewis acidity than the one introduced in the outer O_3O_3 site. At this stage, we had to face the problem coming from the difficult crystallization of these complexes containing three nitrato anions. So, in a following step, we used ^{155}Gd and ^{151}Eu Mössbauer spectrometry in order to confirm that the $LGd(H_2O)Eu(NO_3)_3 \cdot H_2O$ heterodinuclear complex is a pure complex, the Gd^{III} ion being located in the inner N_4O_3 coordination site and the Eu^{III} ion in the outer O_3O_3 coordination site [10]. This result highlights the efficiency of the experimental process for the preparation of heterodinuclear Ln-Ln' complexes, what is quite uncommon for two consecutive Ln ions of the periodic table. We also tried to replace at least one of these nitrato anions by ancillary ligands. And introduction of the ortho-vanillin ligand (ovanH) in place of one nitrato anion allowed us to isolate crystals suitable for the structural determination of the homodinuclear $[LDy(H_2O)Dy(H_2O)(ovan)](NO_3)_2(H_2O)_2$ complex [11]. Following the same experimental process in the present work, we could obtain crystals of other heterodinuclear complexes and study their magnetic properties. But the structural determination of the Lu-Dy complex has given information on the possible replacement of nitrato anions by carbonato anions. Thanks to structural determinations, we could understand that the crystallization time and the role of base in the reaction medium were two factors responsible for this replacement. In view of this problem, we tried to find a new crystallization pathway avoiding base addition. The use of lanthanide chloride salts appeared to be more efficient to obtain crystals of genuine homo and heterodinuclear Lanthanide complexes that were characterized by their structural determinations and some of their magnetic properties.

Experimental Section

Materials. The tripodal LH_3 ligand (Scheme 1) was prepared according to a literature procedure [12]. The mononuclear $LLn.H_2O$ complexes were prepared as previously described [11,13]. Triethylamine, orthovanillin (Hovan), $La(NO_3)_3 \cdot 6H_2O$, $Gd(NO_3)_3 \cdot 5H_2O$, $Dy(NO_3)_3 \cdot 6H_2O$, $Lu(NO_3)_3 \cdot 6H_2O$, $PrCl_3 \cdot 6H_2O$, $NdCl_3 \cdot 6H_2O$, $DyCl_3 \cdot 6H_2O$, $ErCl_3 \cdot 6H_2O$ (Aldrich) were used as purchased. High-grade solvents (methanol, isopropanol, diethyl ether) were used for the syntheses of ligands and complexes. Note that in the dinuclear complexes the lanthanide ion first named is located in the inner N_4O_3 coordination site of the main deprotonated ligand L^{3-} while the following lanthanide ion is positioned in the outer O_3O_3 coordination site, all along the paper. In order to simplify writing and to facilitate understanding, the different species will be abbreviated as follows: DyGd(ovan) for $[LDy(H_2O)Gd(ovan)(H_2O)]$ $(NO_3)_2(H_2O)_4$ and ErDyCl for $[LEr(H_2O)Dy(MeOH)_2Cl](ClO_4)_2$ for example.

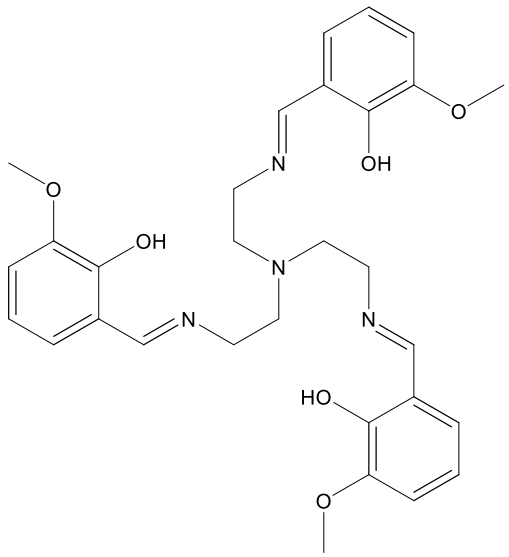

Scheme 1. The tripodal LH_3 ligand used in the preparation of different heterodinuclear Ln–Ln' complexes.

Complexes syntheses.

$[LDy(H_2O)Gd(ovan)(H_2O)](NO_3)_2(H_2O)_4$, DyGd(ovan). $Gd(NO_3)_3 \cdot 5H_2O$ (60 mg, 1.37 10^{-4} mol), Hovan (22 mg,1.38 10^{-4} mol) and tetraethylammonium hydroxide (60 mg, 1.38 10^{-4} mol) were added to a suspension of $LDy.H_2O$ (100 mg, 1.38 10^{-4} mol) in methanol (10 mL) and stirred for 20 min, yielding a yellow solution that was filtered off and reduced to half-volume. Addition of isopropyl alcohol (7 mL) induced formation of a precipitate that was filtered off

and dried. Yield: 87 mg (50 %). Anal. Calcd for $C_{38}H_{52}DyGdN_6O_{21}$ (1248.61 g/mol): C, 36.55; H, 4.20; N, 6.73. Found: C, 36.41; H, 4.14; N, 6.63. IR (ATR): 3411l, 1623s, 1467m, 1443m, 1405m, 1330m, 1240m, 1217m, 1212m, 1082m, 965m, 739m cm^{-1}. FAB^+ (dmf, mnba): 1078 (100).

$[LDy(H_2O)La(ovan)(H_2O)](NO_3)_2(H_2O)_4$, DyLa(ovan). $La(NO_3)_3{\cdot}6H_2O$ (60 mg, 1.38 10^{-4} mol), Hovan (21 mg, 1.38 10^{-4} mol) and tetraethylammonium hydroxide (60 mg, 1.38 10^{-4} mol) were added to a suspension of $LDy.H_2O$ (100 mg, 1.38 10^{-4} mol) in methanol (10 mL) and stirred for 20 min, yielding a yellow solution that was filtered off and reduced to half-volume. Addition of isopropyl alcohol (7 mL) induced formation of a precipitate that was filtered off and dried. Yield: 80 mg (47 %). Anal. Calcd for $C_{38}H_{52}DyLaN_6O_{21}$ (1230.26 g/mol): C, 37.10; H, 4.26; N, 6.83. Found: C, 36.85; H, 4.18; N, 6.58. IR (ATR): 3390l, 1623s, 1467m, 1443m, 1405m, 1330m, 1240m, 1217m, 1212m, 1082m, 965m, 739m cm^{-1}. FAB^+ (dmf, mnba): 1061 (100).

$[LLu(H_2O)Dy(ovan)(H_2O)](NO_3)(CO_3)_{0.5}(H_2O)_3$, LuDy(ovan). $Dy(NO_3)_3{\cdot}6H_2O$ (63 mg, 1.35 10^{-4} mol), Hovan (21 mg,1.35 10^{-4} mol) and tetraethylammonium hydroxide (60 mg, 1.35 10^{-4} mol) were added to a suspension of $LLu.H_2O$ (100 mg, 1.35 10^{-4} mol) in methanol (10 mL) and stirred for 20 min, yielding a yellow solution that was filtered off and reduced to half-volume. Slow evaporation of this mother solution yielded crystals suitable for a X-Ray study. They were isolated by filtration and dried. Yield: 87 mg (52 %). Anal. Calcd for $C_{38.5}H_{50}DyLuN_5O_{18.5}$ (1216.31 g/mol): C, 38.02; H, 4.14; N, 5.76. Found: C, 37.55; H, 4.20; N, 5.73. IR (ATR): 3376l, 1625s, 1605m, 1465m, 1424m, 1331m, 1293s, 1229m, 1209s, 1068m, 956m, 737m cm^{-1}. Crystals were obtained by slow crystallization of the mother solution.

$[LDy(H_2O)Dy(ovan)(H_2O)](CO_3)$, DyDy(ovan). $Dy(NO_3)_3{\cdot}6H_2O$ (63 mg, 1.38 10^{-4} mol), Hovan (21 mg,1.38 10^{-4} mol) and tetraethylammonium hydroxide (60 mg, 1.38 10^{-4} mol) were added to a suspension of $LDy.H_2O$ (100 mg, 1.38 10^{-4} mol) in methanol (10 mL) and stirred for 20 min, yielding a yellow solution that was filtered off and reduced to half-volume. Slow evaporation of this mother solution yielded crystals suitable for a X-Ray study. They were isolated by filtration and dried. Yield: 70 mg (45 %). Anal. Calcd for $C_{39}H_{44}Dy_2N_4O_{14}$ (1117.80 g/mol): C, 41.90; H, 3.97; N, 5.01. Found: C, 41.57; H, 3.81; N, 4.88. IR (ATR): 3395l, 1620s, 1462m, 1416m, 1338m, 1301m, 1290m, 1222m, 1212m, 1072m, 958m, 736m, 729m cm^{-1}.

[LEr(H_2O)Er($MeOH$)$_2$Cl](ClO_4)$_2$($C_4H_{10}O$)(CH_4O)$_2$, ErErCl. $ErCl_3 \cdot 6H_2O$ (30 mg, 8 10^{-5} mol) and $NaClO_4$ (20 mg,1.6 10^{-4} mol) were added to a suspension of LEr.H_2O (50 mg, 6.8 10^{-4} mol) in methanol (10 mL) and stirred for 20 min, yielding a yellow solution that was filtered off and reduced to half-volume. Slow diffusion of diethyl oxide into the solution yielded crystals suitable for a X-Ray study. They were isolated by filtration and dried. Yield: 40 mg (44 %). Anal. Calcd for $C_{32}H_{43}Er_2N_4O_{17}$, ($C_4H_{10}O$)($CH_4O$)$_2$ (1334.80 g/mol): C, 34.19; H, 4.61; N, 4.20. Found: C, 33.85; H, 4.46; N, 4.11. IR (ATR): 3410l, 1657m, 1626s, 1467s, 1291m, 1227m, 1094m, 1067s, 1019m, 739m, 621m cm^{-1}.

[LEr(H_2O)Dy($MeOH$)$_2$Cl](ClO_4)$_2$, ErDyCl. $DyCl_3 \cdot 6H_2O$ (30 mg, 8 10^{-5} mol) and $NaClO_4$ (20 mg,1.6 10^{-4} mol) were added to a suspension of LDy.H_2O (50 mg, 6.8 10^{-4} mol) in methanol (10 mL) and stirred for 20 min, yielding a yellow solution that was filtered off and reduced to half-volume. Slow diffusion of diethyl oxide into the solution yielded crystals suitable for a X-Ray study. They were isolated by filtration and dried. Yield: 42 mg (52 %). Anal. Calcd for $C_{32}H_{43}DyErN_4O_{17}$ (1191.83 g/mol): C, 32.25; H, 3.64; N, 4.70. Found: C, 32.05; H, 3.49; N, 4.51. IR (ATR): 3416l, 1655m, 1625s, 1466s, 1291m, 1228m, 1094m, 1067s, 1017m, 739m, 621m cm^{-1}.

[LDyClDy($MeOH$)$_2$Cl](ClO_4), DyClDyCl. $DyCl_3 \cdot 6H_2O$ (30 mg, 8 10^{-5} mol) and $NaClO_4$ (20 mg,1.6 10^{-4} mol) were added to a suspension of LDy.H_2O (50 mg, 6.8 10^{-4} mol) in methanol (10 mL) and stirred for 20 min, yielding a yellow solution that was filtered off and reduced to half-volume. Slow diffusion of diethyl oxide into the solution yielded crystals suitable for a X-Ray study. They were isolated by filtration and dried. Yield: 35 mg (46 %). Anal. Calcd for $C_{32}H_{41}Dy_2N_4O_{12}$ (1105.06 g/mol): C, 34.78; H, 3.74; N, 5.07. Found: C, 34.55; H, 3.53; N, 4.88. IR (ATR): 3420l, 1653m, 1624s, 1467s, 1292m, 1227m, 1094m, 1067s, 7'àm, 621m cm^{-1}.

[LGd(H_2O)Nd($MeOH$)$_2$Cl](ClO_4)$_2$(CH_4O), GdNdCl. $NdCl_3 \cdot 6H_2O$ (29 mg, 8 10^{-5} mol) and $NaClO_4$ (20 mg,1.6 10^{-4} mol) were added to a suspension of LGd.H_2O (50 mg, 6.9 10^{-4} mol) in methanol (10 mL) and stirred for 20 min, yielding a yellow solution that was filtered off and reduced to half-volume. Slow diffusion of diethyl oxide into the solution yielded crystals suitable for a X-Ray study. They were isolated by filtration and dried. Yield: 39 mg (48 %). Anal. Calcd for $C_{32}H_{43}GdN_4NdO_{17}$,($CH_4O$) (1195.60 g/mol): C, 33.15; H, 3.96; N, 4.69. Found: C, 32.95; H, 3.81; N, 4.50. IR (ATR): 3345l, 1623s, 1460s, 1289m, 1222m, 1096m, 1064s, 1009m, 742m, 621m cm^{-1}.

[LGd(H_2O)Pr($MeOH$)$_2$Cl](ClO_4)$_2$(CH_4O), GdPrCl. $PrCl_3 \cdot 6H_2O$ (29 mg, 8 10^{-5} mol) and $NaClO_4$ (20 mg,1.6 10^{-4} mol) were added to a suspension of LGd.H_2O (50 mg, 6.9 10^{-4} mol) in methanol (10 mL) and stirred for 20 min, yielding a yellow solution that was filtered off and reduced to half-volume. Slow diffusion of diethyl oxide into the solution yielded crystals that were isolated by filtration and dried. Yield: 39 mg (48 %). Anal. Calcd for $C_{32}H_{43}GdN_4PrO_{17}$, ($CH_4O$) (1195.60 g/mol): C, 33.24; H, 3.97; N, 4.70. Found: C, 32.97; H, 3.83; N, 4.52. IR (ATR): 3327l, 1623s, 1460s, 1290m, 1222m, 1096m, 1065s, 1010m, 742m, 621m cm^{-1}.

Physical measurements. C, H, and N elemental analyses were carried out at the Laboratoire de Chimie de Coordination, Microanalytical department, in Toulouse, France. IR spectra were recorded with a Perkin-Elmer Spectrum 100FTIR using the ATR mode. FAB mass spectra were recorded on a Nermag R10-10 spectrometer using dimethylformamide (dmf) as solvent and m-nitrobenzyl alcohol (NBA) as matrix. Magnetic susceptibility data (2-300K) were collected on powdered polycrystalline samples on a Quantum Design MPMS-XL SQUID magnetometer under an applied magnetic field of 0.1 T. *ac* measurements were performed in the 2-11K range using a 3.0 Oe *ac* field oscillation in 1-1500Hz range. Magnetization isotherms were collected at 2, 3, 4, 5K between 0 and 5T. All data were corrected from the sample holder contribution and the diamagnetism of the samples estimated from Pascal's constants [14]. The magnetic hysteresis loops have been measured on single crystals of **1**-**3** using a micro-SQUID technique [15]. The field was aligned with the easy axis of magnetization using a transverse field method [16].

Crystallographic data collection and structure determination for the different complexes.

Crystals were kept in the mother liquor until they were dipped into oil. The chosen crystals were mounted on a Mitegen micromount and quickly cooled down to 180 K (DyDy(ovan) and LuDy(ovan))or 100 K (ErErCl, ErDyCl, DyClDyCl and GdNdCl). The selected crystals of DyDy(ovan) (pale yellow, 0.200 x 0.200 x 0.020 mm^3), LuDy(ovan) (yellow, 0.300 x 0.050 x 0.050 mm^3), GdNdCl (colorless, 0.200 x 0.200 x 0.200 mm^3), ErDyCl (yellow, 0.150 x 0.200 x 0.200 mm^3), ErErCl (yellow, 0.150 x 0.150 x 0.200 mm^3), DyClDyCl (pale green, 0.150 x 0.200 x 0.20 mm^3) were mounted on a Oxford diffraction Gemini (DyDy(ovan), GdNdCl, DyClDyCl), a Bruker Kappa Apex II (LuDy(ovan), ErDyCl, ErErCl) using molybdenum (λ = 0.71073 Å) and equipped with an Oxford Cryosystems cooler device. The unit cell determination and data integration were carried out using CrysAlis RED or SAINT packages [17-19]. The structures have been solved using SUPERFLIP [20] or SHELXS-97 [21] and

refined by least-squares procedures using the software packages CRYSTALS [22] or WinGX version 1.63 [23]. Atomic Scattering Factors were taken from the International tables for X-Ray Crystallography [24]. All hydrogen atoms were refined by using a riding model. When it was possible, all non-hydrogen atoms were anisotropically refined. Drawings of molecules have been performed with the program MERCURY [25]. Cif data for LuDy(ovan), DyDy(ovan), ErDyCl, ErErCl, DyClDyCl, GdNdCl have been deposited at CCDC with references CCDC 2281011-2281016, respectively.

Crystal data for DyDy(ovan): $C_{39}H_{44}Dy_2N_4O_{14}$, M = 1117.80, monoclinic, C2/c, Z = 8, *a* = 38.3454(16), *b* = 11.0104(3), *c* = 24.5964(9) Å, α = γ = 90, β = 118.297(5)°, *V* = 9143.6(7) Å^3, 80972 collected reflections, 11541 unique reflections (R_{int} = 0.0873), R-factor = 0.051, weighted R-factor = 0.054 for 7005 contributing reflections [I > 3σ (I)].

Crystal data for LuDy(ovan): $C_{38.5}H_{50}DyLuN_5O_{18}$, M = 1208.31, monoclinic, C2/c, Z = 8, *a* = 38.1410(17), *b* = 11.0567(5), *c* = 24.3695(11) Å, α = γ = 90, β = 117.724(2)°, *V* = 9097.1(7) Å^3, 80380 collected reflections, 13305 unique reflections (R_{int} = 0.0383), R-factor = 0.043, weighted R-factor = 0.056 for 13269 contributing reflections [I > 2σ (I)].

Crystal data for GdNdCl: $C_{33}H_{47}Cl_3GdN_4NdO_{18}$, M = 1195.60, triclinic, P-1, Z = 2, *a* = 9.83702(15), *b* = 14.6637(2), *c* = 15.2306(2) Å, α = 82.8489(12), β = 89.1141(12), γ = 74.7679(13)° *V* = 2102.95(6) Å^3, 89358 collected reflections, 10449 unique reflections (R_{int} = 0.0349), R-factor = 0.024, weighted R-factor = 0.037 for 8714 contributing reflections [I > 2σ (I)].

Crystal data for ErDyCl: $C_{32}H_{43}Cl_3DyErN_4O_{17}$, M = 1191.83, monoclinic, P2/a, Z = 4, *a* = 14.9805(4), *b* = 21.4567(6), *c* = 15.1544(4) Å, α = γ = 90, β = 99.532(2)°, *V* = 4803.9(2) Å^3, 12785 collected reflections, 12785 unique reflections (R_{int} = 0.0595), R-factor = 0.094, weighted R-factor = 0.094 for 9801 contributing reflections [I > 3σ (I)].

Crystal data for ErErCl: $C_{38}H_{61}Cl_3Er_2N_4O_{20}$, M = 1334.80, monoclinic, P2/c, Z = 4, *a* = 15.1534(7), *b* = 21.5775(10), *c* = 14.9998(7) Å, α = γ = 90, β = 99.156(2)°, *V* = 4842.0(4) Å^3, 78895 collected reflections, 14234 unique reflections (R_{int} = 0.0518), R-factor = 0.065, weighted R-factor = 0.127 for 8714 contributing reflections [I > 3σ (I)].

Crystal data for DyClDyCl: $C_{31.5}H_{40}Cl_3Dy_2N_4O_{12}$, M = 1098.04, monoclinic, P2/c, Z = 4, *a* = 16.34464(13), *b* = 15.18385(12), *c* = 17.23970(15) Å, α = γ = 90, β = 101.3369(8)°, *V* = 4194.97(6) Å^3, 87676 collected reflections, 10467 unique reflections (R_{int} = 0.029), R-factor = 0.024, weighted R-factor = 0.032 for 9078 contributing reflections [I > 3σ (I)].

Results and Discussion

The different homo- and hetero-dinuclear Ln-Ln' complexes are prepared according to a previously reported stepwise process [11] with use of a tripodal ligand reported in Scheme 1. This ligand possesses ten coordinating atoms, four nitrogen and six oxygen atoms, which give an inner N_4O_3 and an outer O_3O_3 coordination sites. Once deprotonated the three central phenol functions allow isolation of pure neutral lanthanide LLn complexes that are used as starting material for the preparation of homo- and hetero-dinuclear complexes, thanks to the deprotonated phenol functions belonging to the two coordination sites that provide a triple bridge between the two Ln ions. In our previous work, the isolated complexes, formulated $LLnLn'(NO_3)_3 \cdot xH_2O$, have been characterized by positive fast-atom bombardment $(FAB)^+$ spectrometry [9] and by ^{151}Eu, ^{166}Er and mainly ^{155}Gd Mössbauer spectroscopy [10] but their crystallization was not possible. Then we found that replacement of one nitrato anion by a deprotonated o-vanillin ligand facilitates crystallization. The efficiency of this reaction pathway has been used in the present work to structurally characterize a family of homo and hetero-dinuclear complexes. At this stage we found that nitrato anions could be replaced by hydroxycarbonato or carbonato anions. Replacing the nitrato anions by chloride anions yielded a new family of complexes. Their structural determinations demonstrate that we are dealing with pairs of homo and hetero-dinuclear complexes that are linked by two Cl…HOMe hydrogen bonds, thus giving tetranuclear entities.

Structural determinations. The cationic species $LLu(H_2O)Dy(ovan)(H_2O)]^{2+}$, appearing in Figure 1, presents large similarities with the previously reported $LDy(H_2O)Dy(ovan)(H_2O)](NO_3)_2(H_2O)_2$ molecule [11]. Although they crystallize in different space groups, C2/c and R-3, they only differ by one of their counter-anions, a nitrate anion being replaced by one-half carbonato anion hydrogen-bridged to two water molecules. The lutecium ion in the inner N_4O_3 coordination site is linked to the seven donor atoms of the tripodal ligand and to the oxygen atom of a water molecule (eight-coordinate) while the dysprosium ion is nine-coordinate to oxygen atoms, six coming from the outer O_6 ligand coordination site, two belonging to the aldehyde and deprotonated phenol function of the ancillary orthovanillin ligand and the last one from a water molecule. The central core of the cationic unit is made of a triply phenoxo-bridge linking the lutecium and dysprosium ions, with a separation equal to 3.4979(3) Å. As expected the Lu-O and Lu-N bond lengths are shorter than the Dy-N and Dy-O bond lengths for ions in the inner N_4O_4 site, which induces shorter intramolecular Lu…Dy (3.4979(3) Å) in comparison to the Dy…Dy one (3.5214(2) Å). Each

ion is coordinated to a water molecule (2.315(3) and 2.399(3) Å for Lu and Dy respectively). They are located on the same side of the molecule for they are hydrogen-bonded to two different oxygen atoms of the nitrato anion. Note that the shortest Ln-O bond is the Dy-O bond involving the phenoxo oxygen atom of the ovan ancillary ligand with a bond length of 2.188(3) Å. The shortest intermolecular Dy…Dy distance is larger than 9 Å (9.382(1) Å), so that complex LuDy(ovan) may be considered as a genuine example of strictly dinuclear Lu^{III}-Dy^{III} species.

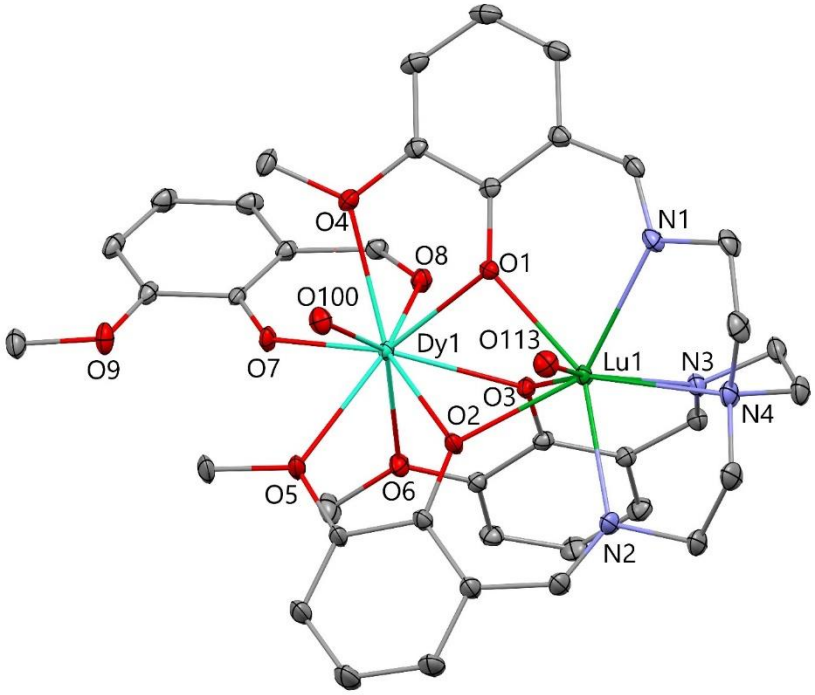

Figure 1. View of the cationic $LLu(H_2O)Dy(ovan)(H_2O)]^{2+}$ entity.

There are no large differences in the present $LDy(H_2O)Dy(ovan)(H_2O)](CO_3)$ complex (Figure S1) and the previously published complex, except that the carbonato anion replaces the two nitrato anions. The main difference comes from the hydrogen bond network, which is more developed in the nitrato complex, due to the presence of two anionic NO_3 anions and two crystallization water while it is limited to the coordinated water molecules which are hydrogen-bonded to two different oxygen atoms of the carbonato anion. If the intramolecular distance is quite similar (3.5214(2) and 3.5196(3) Å), the intermolecular Dy-Dy distance of the outer Dy ions slightly increases from 8.302(1) to 9.324(1) Å in the carbonato complex. The Dy-Ow bond lengths (2.314(4) and 2.401(3) Å for Dy2 and Dy1 respectively) are equivalent to the Dy-$O_{phenoxo}$ bond lengths of the main ligand.

The complexes prepared by use of chloride salts crystallize in the monoclinic $P2_1/c$ (ErErCl, DyClDyCl) or $P2_1/a$ (ErDyCl) space groups, except for complex (GdNdCl) that crystallizes in the triclinic P^{-1} space group. It has to be noted that the complexes involving Ln ions of the

second half of the series crystallize in monoclinic space groups while the one involving Ln ions of the first half of the series crystallizes in a triclinic space group. These cationic species are formulated $[LLn(H_2O)Ln'Cl(MeOH)_2]^{2+}$ (Ln = Gd, Er; Ln' = Nd, Dy, Er), at the exception of complex $[LDyClDyCl(MeOH)_2]^{+}$ in which a chloride ligand replaces the water molecule coordinated to the inner Dy ion. As an example, a view of the ErDyCl complex is reported on Figure 2 while the views of the other complexes are reported in the Supplementary Information (Figures S2 for ErErCl, S3 for DyClDyCl, S4 forGdNdCl). In comparison to the previous structures LuDy(ovan) and DyDy(ovan), the main changes concern the Ln ion in the outer coordination site, which becomes coordinated to a chloride ligand and two oxygen atoms coming from two methanol molecules, without any change of the coordination number of the two Ln ions, respectively eight- and nine-coordinate. We still have dicationic species with two perchlorato anions in place of nitrato, hydrocarbonato or carbonato anions, except for the monocationic DyClDyCl compound, in which the water molecule linked to the inner Dy ion is replaced by a chloride ligand. Concerning the bond lengths, it is clear that the Ln-Cl bonds (2.6804(6)-2.7648(6) Å) are larger than the Ln-O(phenolato) (2.190(3)-2.199(3) Å) for the outer Ln ion while the other Ln-O and Ln-N bond lengths are quite comparable for the inner and outer Ln ions (Table S1). As a consequence the Ln…Ln intramolecular distances are quite identical in the two series of complexes and they slightly vary according to the Ln contraction, 3.4979(3) Å for the LuDy(ovan) pair and 3.6396(2) Å for the GdNdCl pair. Two intermolecular Cl…H-OMe hydrogen bonds assemble two cationic species, thus introducing an intermolecular Ln..Ln distance involving the Ln ions located in the outer coordination site of ~7 Å (Er…Er = 6.997(1) Å for ErErCl, Er…Dy = 7.004(1) Å for ErDyCl (Figure S5), Dy…Dy = 7.107(1) Å for DyClDyCl, Nd…Nd = 6.968(1) Å for GdNdCl). The other intermolecular Ln…Ln distances are larger than 10 Å.

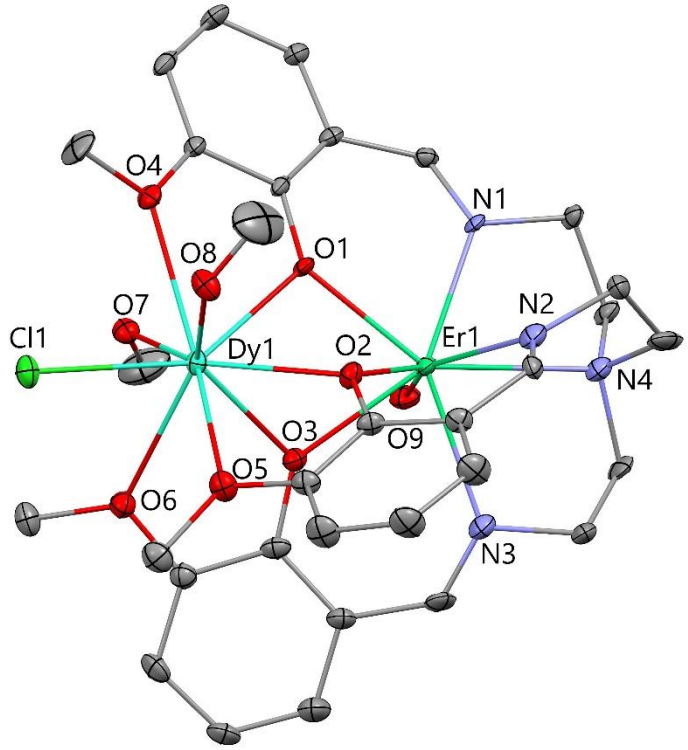

Figure 2. View of the cationic $[LEr(H_2O)DyCl(MeOH)_2]^{2+}$ entity.

Application of the "SHAPE" program [26] indicates that the nine-coordinate Dy ions in the outer O_3O_3 coordination spheres are in a slightly deformed spherical tricapped trigonal prism geometry, with small values for the shape measure parameter S_{TCTPR}, equal to 0.66 and 0.68 for complexes LuDy(ovan) and DyDy(ovan) respectively. The coordination spheres of the LErErCl and ErDyCl complexes are best represented by spherical capped square antiprism environments in a very slightly larger deformation with S_{CSAPR} equal to 0.91 and 0.96 respectively while the muffin geometry corresponds to the best environment for the LDyClDyCl and LGdNdCl complexes, with S_{MFF} values of 0.99 and 1.13. We can note that these deformations are not far from the corresponding regular polyhedral. On the opposite, the eight-coordinate Ln ions in the inner coordination sites present larger deformations from the regular biaugmented trigonal prism polyhedron, with S_{BTPR} values going from 1.99 to 2.63 (Table S2).

Magnetic properties.

The magnetic susceptibilities of the dinuclear LuDy(ovan), DyLa(ovan), DyGd(ovan) and DyDy(ovan) complexes have been measured in the 2-300 K temperature range in a 0.1 T applied magnetic field along with the field dependence of the magnetization M at 2 K and a 5 T magnetic field. At 300 K, the $\chi_M T$ is equal to 13.9 $cm^3mol^{-1}K$ for the LuDy(ovan) complex, in agreement with the expected value for an isolated Dy^{III} uncoupled ions (14.2 $cm^3mol^{-1}K$). Lowering the temperature causes $\chi_M T$ to decrease smoothly to a value of 12.3 $cm^3mol^{-1}K$

(Figure S6) at 2 K while the saturation value of magnetization at 5 T is equal to 5.6 Nβ, far from the expected value of 10 Nβ (Figure S7). For the DyLa(ovan) entity, the $\chi_M T$ value at 300 K equals 13.3 $cm^3mol^{-1}K$ but the temperature decrease induces a larger $\chi_M T$ decrease to 7.8 $cm^3mol^{-1}K$ (Figure S8). The magnetization value at 5 T (5.4 Nβ) is again far from the expected value (Figure S9). In the case of the DyGd(ovan) complex, the $\chi_M T$ value at 300 K (21.1 $cm^3mol^{-1}K$) is slightly lower than expected (22.0 $cm^3mol^{-1}K$). A larger decrease follows the temperature decrease, a value of 13.7 $cm^3mol^{-1}K$ being observed at 2 K (Figure S10). The magnetization value at 5 T and 2 K (12.9 Nβ) is again far from the expected 17 Nβ value (Figure S11). A slightly different behaviour is found for the Dy-Dy complex (Figure 3). The $\chi_M T$ decrease from 300 K (27.2 $cm^3mol^{-1}K$) to 4 K (21.5 $cm^3mol^{-1}K$) is followed by a very weak increase (21.7 $cm^3mol^{-1}K$) but the magnetization value at 5 T and 2 K (11.6 Nβ) is again far from the expected 20 Nβ value (Figure S12). Starting with the $\chi_M T$ curves of these four complexes, it is possible to determine the Dy-Gd and Dy-Dy exchange interactions by use of the diamagnetic substitution method [9,27]. Subtracting the temperature-dependent contribution arising from the thermal depopulation of the excited levels of the Dy^{III} ion furnished by the Dy-La complex from the $\chi_M T$ curve of the exchange-coupled Dy-Gd complex (Figure S13), confirms that an antiferromagnetic Dy-Gd interaction is active. According to the same process, a comparison of the $\chi_M T$ curve corresponding to the sum of the Dy-La and Lu-Dy contributions with the $\chi_M T$ curve of the Dy-Dy complex allows to understand that the lower $\chi_M T$ decrease must be due to the presence of a ferromagnetic Dy-Dy interaction (Figure S14) but we have not tried to quantify its value according to the approach recently described [28].

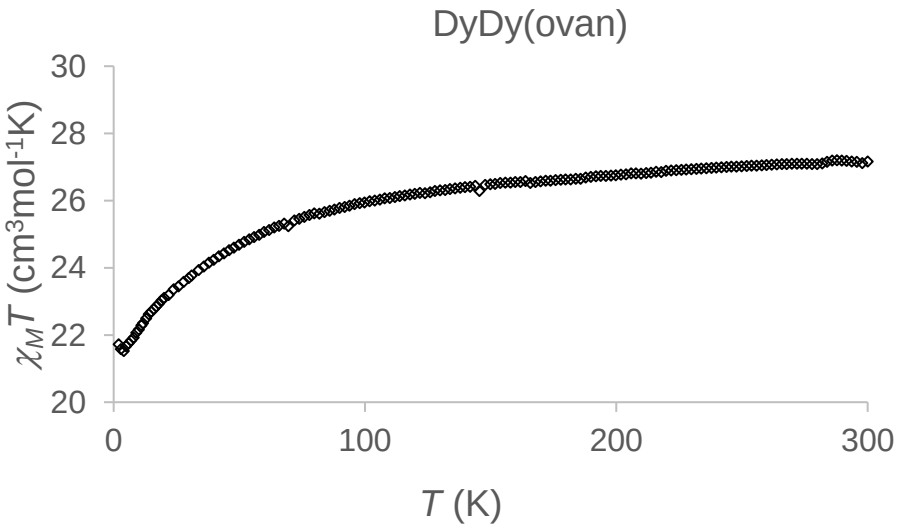

Figure 3. Temperature dependence of the $\chi_M T$ product for DyDy(ovan) at 0.1 T applied magnetic field.

Similar measurements have been made for the complexes involving chloride ions. For the ErDyCl complex, the $\chi_M T$ product is equal to 25.3 $cm^3mol^{-1}K$ at 300K. This value, which remains constant till 80 K, is followed by a slight decrease to 22.6 $cm^3mol^{-1}K$ at 20 K and eventually by a more abrupt decrease to 15.5 $cm^3mol^{-1}K$ at 2 K (Figure S15). The magnetization value at 5 T and 2 K (11.9 Nβ) is again far from the expected 19 Nβ value (Figure S16). In the case of the GdNd complex, we observe a slight decrease of the $\chi_M T$ product from 9.9 $cm^3mol^{-1}K$ at 300 K to 9.1 $cm^3mol^{-1}K$ at 7 K, followed by a slight increase to 9.6 $cm^3mol^{-1}K$ at 2 K (Figure 4). The magnetization value at 5 T and 2 K is again lower than expected, 8.7 Nβ instead of 10.3 Nβ (Figure S17). For the GdPrCl complex, we observe a slight decrease of the $\chi_M T$ product from 9.2 $cm^3mol^{-1}K$ at 300 K to 8.6 $cm^3mol^{-1}K$ at 19 K, followed by a more pronounced decrease to 7.9 at 3 K and a very slight increase to 8.0 $cm^3mol^{-1}K$ at 2 K (Figure S18) and a magnetization value at 5 T and 2 K equal to 7.4 Nβ instead of the expected value of 10.2 Nβ (Figure S19). These experimental values are in favor of an antiferromanetic Er-Dy interaction, in agreement with previous ^{166}Er Mössbauer data dealing with a Er-Gd complex, while a weak ferromagnetic Gd-Nd interaction seems to be active at low temperature. By analogy to the GdNdCl complex, a similar interaction is expected in the GdPrCl complex. In the entire set of complexes, the field dependence of the different magnetization plots are very similar, with a rapid increase at low field followed by a nearly linear and slow increase to values at 5 T that are lower than the expected saturation values. Such a behavior must be due to crystal-field effects leading to significant magnetic anisotropy.

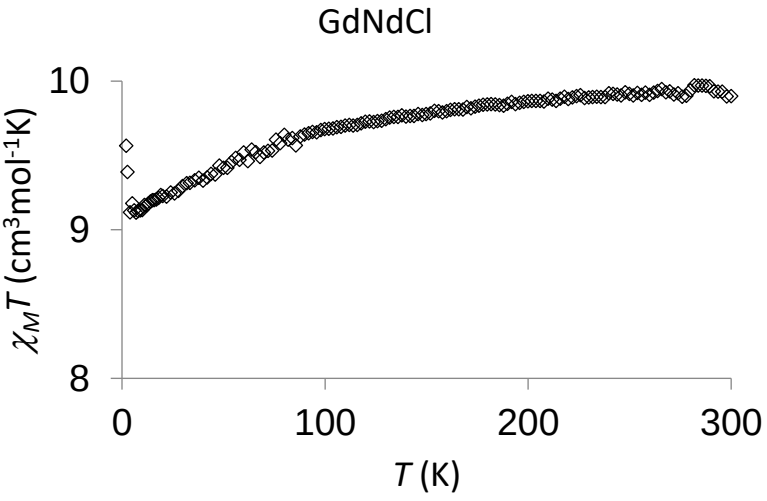

Figure 4. Temperature dependence of the $\chi_M T$ product for GdNdCl at 0.1 T applied magnetic field.

Preliminary dynamic ac magnetic susceptibility measurements as a function of the temperature and frequencies (99.9, 997 and 1490 Hz) were performed on microcrystalline powder samples of the different complexes. Below 5 K, out-of-phase signals χ''_M are observed under zero external field, without appearance of maxima (Figures S20, S21), except for the DyDy(ovan) sample where a bump appeared around 7 K (Figure S22). These signals are attributed to the presence of a fast relaxation of the magnetization through a quantum tunneling mechanism. Performing these ac susceptibility measurements in the presence of an external dc field of 2000 Oe, bumps are seen at 5 and 11 K (1490 Hz) for the DyDy(ovan) sample (Figure S23) and at 7 K (1490 Hz) for the DyGd(ovan) sample (Figure S24). But two out-of-phase peaks in the 4.5 K–8 K (99.9 Hz) range and 5 K–12 K (1490 Hz) range are observed for the Lu-Dy sample (Figure S25). According to these results, we can tell that the only complexes that show a SMM behavior are the Lu-Dy and Dy-Dy ones, the best one being the Lu-Dy complex but it is clear that the quantum tunneling of magnetization has not been efficiently suppressed, even in the Lu-Dy case. For the GdNdCl and GdPrCl samples out-of-phase signals χ''_M are observed without appearance of maxima, even in the presence of an external dc field of 1000 Oe (Figures S26, S27).

We used therefore a micro-SQUID apparatus [15] to study the magnetization dynamics down to 0.03 K. The studies were performed on single microcrystals, which were thermalized using Apiezon grease [16]. The field was aligned with the easy axes of magnetization using the transverse field method [16] Figure 5 and Figures S28-S29 show magnetization versus magnetic field hysteresis loops for a single crystal of DyDy(ovan) (left) and DyGd(ovan)

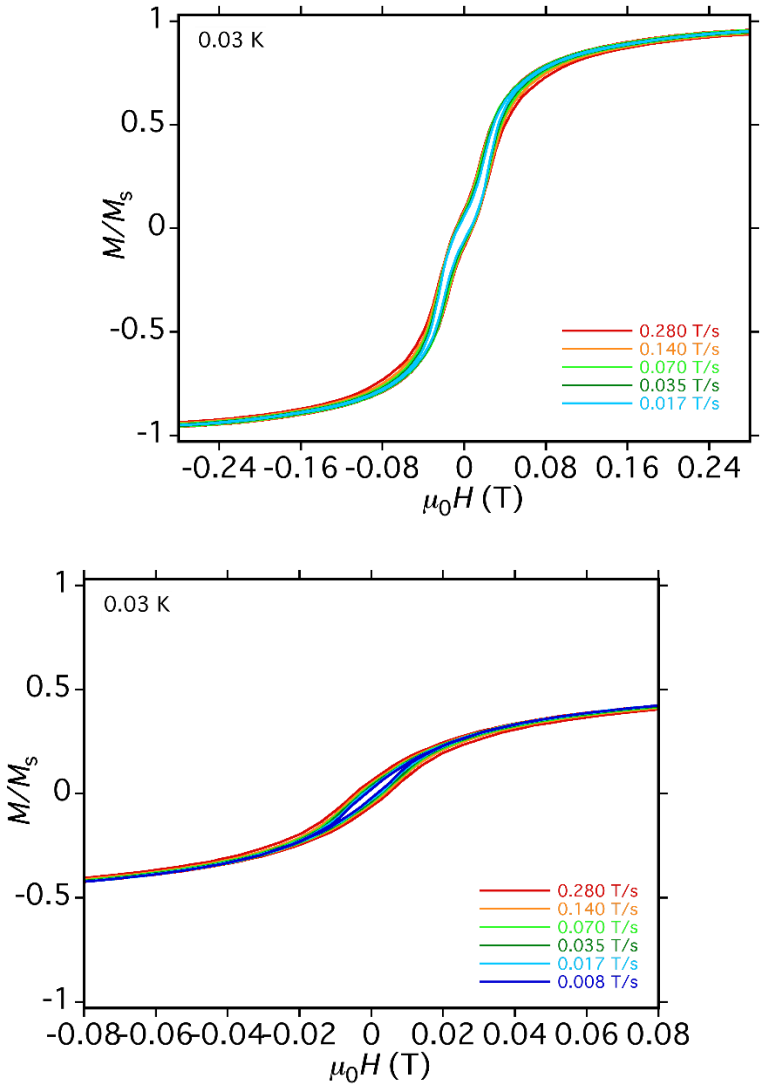

Figure 5. Magnetization *M* versus applied dc field *H* hysteresis loops for single crystals of DyDy(ovan) (left) and DyGd(ovan) (right) at 0.03K for several field sweep rates. The magnetizations are normalized to their saturation values at 1.4 T.

(right) at 0.03 K and different field sweep rates. Narrow hysteresis loops, observed below 0.2 K whose coercivity is temperature and sweep-rate dependent, increasing with decreasing temperature and increasing field sweep rate, do agree with a slow relaxation of magnetization and confirm the superparamagnetic-like behavior of complexes Dy-Dy(ovan) and Dy-Gd(ovan), as expected for an SMM below its blocking temperature. The main remark we can do is that these narrow cycles are present only in the samples where weak intramolecular magnetic interactions are active, whatever the sign of the interaction, ferromagnetic (Dy-Dy(ovan)) or antiferromagnetic (Dy-Gd(ovan)). The presence of two exchange coupled lanthanide ions can be seen as the source of a small effective field, able to suppress quantum

tunneling of the magnetization in zero external applied field, leading to effective bistability of the magnetization in zero field. In the Lu-Dy(ovan) sample, in which the Dy ion is associated to a diamagnetic Lu ion, such a magnetic interaction is not present and the loops collapse at zero field (Figure S28). The hysteresis loops of the Dy-Dy(ovan) sample show a "double-S-like" curve, which is characteristic for small antiferromagnetic interactions between molecules. The other studied complexes Dy-La(ovan) (Figure S29), Gd-PrCl (Figure S30), Gd-NdCl (Figure 31), made of a unique anisotropic ion, do not exhibit hysteresis loops, even at 0.03 K. They cannot be considered as SMMs. It is surprising to see that the Gd-NdCl, Gd-PrCl samples, where slight ferromagnetic Gd-Nd and Gd-Pr interactions are active, are devoid of hysteresis loops. If we remember that two hydrogen bonds introduce a double link in between the Pr or Nd ions coordinated in the outer pockets, we can expect that a supplementary Nd-Nd or Pr-Pr interaction through these hydrogen bonds is active, surely antiferromagnetic in nature, thus impeding suppression of quantum tunneling of the magnetization at zero field.

The ac and micro-SQUID measurements do confirm that it is necessary to introduce the Dy ions in the outer oxygenated pocket to favor SMM properties of the resulting dinuclear complexes. By use of the present tripodal ligand, this study indicates that only four heterodinuclear complexes based on Dy ions would present an interest from that point of view, namely the Ho-Dy(ovan), Er-Dy(ovan), Tm-Dy(ovan) and Yb-Dy(ovan) compounds.

Discussion.

The first different homo- and hetero-dinuclear Ln-Ln' complexes that were prepared in a stepwise process [11] with use of the tripodal ligand reported in Scheme 1 were formulated $LLnLn'(NO_3)_3$. As we were not able to obtain crystals suitable for X-Ray study, these complexes have been first characterized by their positive fast-atom bombardment $(FAB)^+$ spectra in meta-nitrobenzyl alcohol matrices, due to the rich isotopic family of Ln ions [9,10]. This study allowed us to demonstrate that pure heterodinuclear Ln-Ln' complexes are isolated if the Ln ion present in the inner N_4O_3 coordination site is a better Lewis acid than the one introduced in the outer O_3O_3 site [9]. Then supplementary information has been furnished by use of ^{151}Eu, ^{166}Er and mainly ^{155}Gd Mössbauer spectroscopy. These Mössbauer results highlight existence of a pure and unique heterodinuclear Gd-Eu complex involving two consecutive ions of the periodic table and confirm presence of an antiferromagnetic interaction in the genuine Er-Gd complex [10]. They also bring an experimental proof for the presence of a partial covalent character corresponding to a partial occupation of the 6s orbitals when the

Gd^{III} ion is in the inner N_4O_3 coordination site while an ionic character is prevailing for Gd^{III} ion in the outer coordination site [10].

A structural determination involving an homodinuclear $[LDy(H_2O)Dy(ovan)(H_2O)](NO_3)_2(H_2O)_2$ complex [11] has been first obtained after introduction of an ancillary ovan (deprotonated orthovanillin) ligand in the coordination sphere of the outer Dy ion. We have tried to develop this strategy to isolate similar heterodinclear complexes. For a better understanding of the magnetic behavior, it is interesting to associate a diamagnetic ion with a magnetic one. This is why we first tried to work with Yttrium ions. According to its ionic radius, the Y^{III} ion is supposed to be assimilated to the Ho^{III} ion. But the FAB^+ mass spectrum of the supposed $LY(H_2O)Dy(ovan)(H_2O)(NO_3)_2$ species does confirm presence of the expected YDy(ovan) monocationic species as the main product associated with the homodinuclear YY(ovan) and DyDy(ovan) cations (Figure S32). This result is slightly different from those obtained with the lanthanide series. As an example, the FAB^+ spectrum of the $LGdDy(NO_3)_3$ complex, in which the Dy ion is a better Lewis acid than the Gd ion, only gives the main cationic $GdDy(NO_3)_2$ product with the homodinuclear $DyDy(NO_3)_2$ one but without the $GdGd(NO_3)_2$ cation. A scrambling reaction does occur in the present case, mainly due to the higher Lewis acid character of the Y ion in comparison to the Dy ion. This result confirms our previous observations and highlights the importance of the ionic radius and the Lewis acid strength in the preparation of pure heterodinuclear Ln-Ln' complexes with our tripodal ligand. So we retained Lu^{III} and La^{III} ions to introduce diamagnetic ions in the inner and outer coordination sites, respectively. As expected, the FAB^+ spectra of the Lu-Dy(ovan), Dy-La(ovan), Dy-Gd(ovan) complexes yielded signals corresponding to the cationic $[LLuDy(ovan)(NO_3)]^+$, $[LDyLa(ovan)(NO_3)]^+$ and $[LDyGd(ovan)(NO_3)]^+$ formulae with maxima of the isotopic pleiades centered at m/z = 1097, 1061 and 1078 uma respectively (Figures S33-S35).

These structural determinations give a supplementary information for the characterization of these complexes. A quick precipitation of these species by use of isopropyl alcohol allows isolation of complexes possessing two nitrato counter-ions while a slower crystallization shows the replacement of a nitrato anion by a hydroxycarbonato or carbonato anion. And by use of an excess of base, we can replace the two nitrato anions by a carbonato anion. The two active factors in these anions replacements are the crystallization time and the presence of base in excess, in complete agreement with previous observations [29]. In order to eliminate such a problem, we tried to find a novel strategy for the preparation of genuine heterodinuclear Ln

complexes. This was successfully accomplished by simple addition of lanthanide chloride salts to the mononuclear LLn complexes in presence of perchlorate anions. So nice crystals were isolated more easily. Their structural determinations allowed to characterize new complexes formulated $[LLn(H_2O)Ln'Cl(MeOH)_2](ClO_4)_2$ in the case of ErErCl, ErDyCl and GdNdCl pairs. A water molecule is again coordinated to the Ln ion in the inner N_4O_3 coordination site, except for the DyClDyCl complex, where it is replaced by a chloride ligand. The Ln ion in the outer O_3O_3 site is now surrounded by two methanol molecules and a chloride ligand. As an example, two cationic $[LErDyCl(MeOH)_2]^{2+}$ species are assembled by two intermolecular Cl…H-OMe hydrogen in order to yield tetranuclear $LEr(H_2O)Dy(MeOH)_2Cl…(MeOH)_2ClDy(H_2O)ErL$ compounds, in which a supplementary Dy…Dy magnetic interaction is superimposed to the intramolecular Er-Dy magnetic interactions. Such an interaction could be of interest in the preparation of genuine qubits.

According to the magnetic results, weak ferromagnetic interactions are observed in the DyDy(ovan), GdNdCl and GdPrCl compounds while weak antiferromagnetic interactions are active in the other samples. So, it appears that the association of Gd ions with Ln ions having less than seven f electrons (large Ln ions) does favor a weak ferromagnetic interaction while the association of Gd ions with Ln ions having more than seven f electrons (small Ln ions) induces an antiferromagnetic interaction. This behavior is different from the one observed in 3d-4f complexes but this is not surprising if we remember the main role held by the 3d transition metal orbitals [30]. It seems dangerous to highlight such a simple conclusion but it is interesting to note that the presence of two exchange coupled lanthanide ions can be seen as the source of a small effective field, able to suppress quantum tunneling of the magnetization in zero external applied field. Whatever the sign of the interaction, small hysteresis loops have been observed in the Dy-Dy(ovan) and Dy-Gd(ovan) samples at very low temperature while such cycles do not appear in the LuDy(ovan) and DyLa(ovan) samples, in which Dy ions are associated to diamagnetic La or Lu ions. Unfortunately the GdNdCl, GdPrCl samples, where slight ferromagnetic Gd-Nd and Gd-Pr interactions are active, are devoid of hysteresis loops. We have shown, thanks to the structural determinations, that these complexes are not so well isolated from each other than the ones containing ancillary ovan ligands. We can expect that supplementary Pr-Pr or Nd-Nd interactions through the two hydrogen bonds introducing a double link in between the Pr or Nd ions are active, and that the combination of these intermolecular interactions, surely antiferromagnetic in nature, with the intramolecular Gd-Pr or Gd-Nd interactions would be responsible for the absence of hysteresis loops.

Conclusion

The structural determinations and the magnetic studies of homo and heterodinuclear do confirm the possible association of Ln ions very close in the lanthanide series. Replacement of a nitrato anion by an ancillary deprotonated ovan ligand allows isolation and structural determinations of well separated homo and hetero-dinuclear complexes. It has been possible to understand why the non coordinated nitrato anions can be replaced by hydroxycarbonato or carbonato anions. If a quick precipitation favours formation of the expected compound with two non coordinated nitrato anions, a longer crystallization time in basic solvent medium induces replacement of one or two nitrato anions by hydroxycarbonato or carbonato anions. In the absence of nitrato anions, an easier crystallization mode has been evidenced but the structural determination indicates that the resulting complexes are teranuclear, two dinuclear entities being linked together by two intermolecular Cl…HOMe hydrogen bonds involving Cl and MeOH molecules coordinated to the Ln ion located in the outer O_3O_3 coordination site of the main ligand. Furthermore the presence of two exchange coupled lanthanide ions creates a small effective field that is able to suppress quantum tunneling of the magnetization in zero external applied field. So hysteresis loops appear at very low temperature in the well isolated DyDy(ovan) and DyGd(ovan) complexes, whatever the sign of the intramolecular Dy-Dy or Dy-Gd interaction. Among these complexes, the presence of a Dy ion in the outer coordination sphere does favor the SMM property, as in the DyDy(ovan) and LuDy(ovan) complexes. Eventually the two preparation pathways described in the present work will be able to give novel and genuine examples of homo and hetero-dinuclear and tetranuclear lanthanide complexes likely to furnish coordination complexes useful in quantum computing.

Appendix A. Supplementary data. CCDC contains the supplementary crystallographic data for LuDy(ovan), DyDy(ovan), ErDyCl, ErErCl, DyClDyCl, GdNdCl have been deposited at CCDC with references CCDC 2281011-2281016, respectively. These data can be obtained free of charge via http://www.ccdc.cam.ac.uk/conts/retrieving.html, or from the Cambridge Crystallographic Data Centre, 12 Union Road, Cambridge CB2 1EZ, UK; fax: (+44) 1223-336-033; or e-mail: deposit@ccdc.cam.ac.uk.

Acknowledgements

The authors are grateful to J.-F. Meunier (Laboratoire de Chimie de Coordination) for his technical assistance in recording magnetic data. This work was supported by the European

Union sixth framework program NMP3-CT-2005-515767 entitled “MAGMANet: Molecular Approach to Nanomagnets and Multifunctional Materials”.

References

[1] M. A. Nielsen and I. L. Chuang, Quantum Computation and Quantum Information, Cambridge University Press, 2000.

[2] D. Loss and D. P. Di Vincenzo, Quantum computation with quantum dots, Phys. Rev. A, 57 (1998) 120-126.

[3] J. Lehmann, A. Gaita-Arino, E. Coronado and D. Loss, Spin qubits with electrically gated polyoxometalate molecules, Nat. Nanotechnol. 2 (2007) 312–317.

[4] I. L. Chuang, L. M. K. Vandersypen, X. L. Zhou, D. W. Leung, S. Lloyd, Experimental realization of a quantum algorithm, Nature, 393 (1998) 143-146.

[5] G. Aromi, D. Aguila, P.Gamez, F. Luis, O. Roubeau, Design of magnetic coordination complexes for quantum computing, Chem. Soc. Rev. 41 (2012) 537–546.

[6] D. Aguila, L. A. Barrios, V. Velasco, O. Roubeau, A. Repolles, P. J. Alonso, J. Sese, S. J. Teat, F. Luis, G. Aromí, Heterodimetallic [LnLn′] Lanthanide Complexes: Toward a Chemical Design of Two-Qubit Molecular Spin Quantum Gates, J. Am. Chem. Soc. 136 (2014) 14215−14222.

[7] J. Gónzalez-Fabra, N.A.G. Bandeira, V. Velasco, L.A. Barrios, D. Aguilà, S.J. Teat, O. Roubeau, C. Bo, G. Aromí, Chem. Eur. J. 23 (2017) 5117-5125.

[8] L. Abad Galán, D. Aguilà, Y. Guyot, V. Velasco, O. Roubeau, S. J. Teat, M. Massi, G. Aromí, Chem. Eur. J. 27 (2021) 7288-7299.

[9] J.-P. Costes, F. Nicodème, Unequivocal Synthetic Pathway to Heterodinuclear (4f,4f_) Complexes: Magnetic Study of Relevant (LnIII, GdIII) and (GdIII, LnIII) Complexes, Chem. Eur. J. 8 (2002) 3442−3447.

[10] J.-P. Costes, F. Nicodème, T. Ayabe, M. Takeda, M. Takahashi, Use of 155Gd, 151Eu, 166Er Mössbauer spectroscopy to characterize heterodinuclear Ln–Ln0 complexes, Polyhedron 174 (2019) 114154.

[11] J.-P. Costes, F. Dahan, F. Nicodème, Structure-Based Description of a Step-by-Step Synthesis of Homo- and Heterodinuclear (4f, 4f ¢) Lanthanide Complexes, Inorg. Chem. 42 (2003) 6556−6563.

[12] S. Liu, L. W. Yang, S. J. Rettig, C. Orvig, Bulky Ortho 3-Methoxy Groups on N4O3 Amine Phenol Ligands Producing Six-Coordinate Bis(ligand)lanthanide Complex Cations [Ln(H&)2I3+ (Ln = Pr, Gd; H& = Tris(((2-hydroxy-3-methoxybenzy1)amino)ethyl)amine), Inorg. Chem. 32 (1993) 2773−2778.

[13] E. Lucaccini, J. J. Baldoví, L. Chelazzi, A. L. Barra, F. Grepioni, J. P. Costes, L. Sorace, Electronic Structure and Magnetic Anisotropy in Lanthanoid Single-Ion Magnets with C_3 Symmetry: The Ln(trenovan) Series, Inorg. Chem. 56 (2017) 4728−4738.

[14] P. Pascal, Magnetochemical studies. Annales de Chimie et de Physique, 19 (1910**)** 5-70.

[15] W. Wernsdorfer, Classical and Quantum Magnetization Reversal Studied in Nanometer-Sized Particles and Clusters, Adv. Chem. Phys. 118 (2001) 99.

[16] W. Wernsdorfer, N. E. Chakov, G. Christou, Determination of the magnetic anisotropy axes of single-molecule magnets, Phys. Rev. B, 70 (2004) 132413.

[17] Agilent Technologies, Xcalibur CCD system, CrysAlisPro Software system, Version 1.171.35.19, Agilent Technologies UK Ltd, Oxford, UK, 2011.

[18] CrysAlis CCD, CrysAlis RED and associated programs: Oxford Diffraction. Program name(s). Oxford Diffraction Ltd, Abingdon, England, 2006.

[19] SAINT Bruker, Bruker AXS Inc., Madison, Wisconsin, USA, 2007.

[20] Superflip L. Palatinus and G. Chapuis, J. Appl. Crystallogr. 40 (2007) 786–790.

[21] G. M. Sheldrick, SHELX97 [Includes SHELXS97, SHELXL97, CIFTAB] – Programs for Crystal Structure Analysis (Release 97-2), Institüt für Anorganische Chemie der Universität, Tammanstrasse 4, D-3400 Göttingen, Germany, 1998.

[22] CRYSTALS: P. W. Betteridge, J. R. Carruthers, R. I. Cooper, K. Prout and D. J. Watkin, J. Appl. Crystallogr. 36 (2003) 1487.

[23] WINGX – 1.63 Integrated System of Windows Programs for the Solution, Refinement and Analysis of Single Crystal X-Ray Diffraction Data. L. Farrugia, J. Appl. Crystallogr. 32 (1999) 837–840.

[24] International Tables for X-ray Crystallography, Kynoch Press, Birmingham, England, vol. IV, 1974.

[25] Mercury 2022.2.0 (Build 353591).

[26] M. Llunell, D. Casanova, J. Cirera, J., J. M. Bofill, P. Alemany, S. Alvarez, M. Pinsky, D. Avnir, D. SHAPE, v1.1b; University of Barcelona: Barcelona, Spain, 2005.

[27] D. Gatteschi, R. Sessoli, L. Sorace, Handbook on the Physics and Chemistry of Rare Earths, Volume 50, 2016, Pages 91-139.

[28] S. Dey, G. Rajaraman, An approach to estimate the barrier height for magnetisation reversal in {Dy2} SMMs using ab initio calculations, Dalton Trans. 49 (2020) 14781-14785.

[29] B. El Rez, J. P. Costes, C. Duhayon, L. Vendier, J. P. Sutter, Structural determinations of carbamato-bridging ligands derived from atmospheric CO2 in 3d–4f complexes, Polyhedron 89 (2015) 213–218.

[30] N. Ahmed, T. Sharma, L. Spillecke, C. Koo, K. U. Ansari, S. Tripathi, A. Caneschi, R. Klingeler, G. Rajaraman, M. Shanmugam, Probing the Origin of Ferro-/Antiferromagnetic Exchange Interactions in Cu(II)−4f Complexes, Inorg. Chem. 61 (2022) 5572-5587.